Tectonophysics 622 (2014) 122–134

Contents lists available at ScienceDirect

Tectonophysics

journal homepage: www.elsevier.com/locate/tecto

Vent distribution in the Quaternary Payún Matrú Volcanic Field, western Argentina: Its relation to tectonics and crustal structures

I.R. Hernando [a,*], J.R. Franzese [a], E.J. Llambías [a], I.A. Petrinovic [b]

[a] Centro de Investigaciones Geológicas, Universidad Nacional de La Plata, CONICET, 1 No. 644, La Plata B1900TAC, Argentina
[b] Centro de Investigaciones en Ciencias de la Tierra, Universidad Nacional de Córdoba, CONICET, Av. Vélez Sarfield 1611, Córdoba X5016GCA, Argentina

ARTICLE INFO

Article history:
Received 10 December 2013
Received in revised form 24 February 2014
Accepted 3 March 2014
Available online 11 March 2014

Keywords:
Vent alignments
Horizontal stresses
Pre-existing structures
Payún Matrú caldera

ABSTRACT

The Payún Matrú Volcanic Field consists of two polygenetic and mostly trachytic volcanoes (Payún Matrú with a summit caldera and Payún Liso) along with around 220 scoria cones and basaltic lava flows. This volcanic field belongs to the Payenia Basaltic Province (33° 30′–38° S), a Quaternary Andean back-arc basaltic province of the Southern Volcanic Zone, in western Argentina. The vent density distribution of the Payún Matrú Volcanic Field is different from the other volcanic fields within Payenia. The Payún Matrú volcano and the scoria cones are distributed in an E–W oriented fringe about 15 km wide and 70 km long, with the Payún Matrú caldera in the middle of this fringe. The structural framework in which the volcanic field is located allows to infer that this vent density distribution is strongly conditioned by pre-existing crustal anisotropies. The volcanic field is located in a transfer zone related to Jurassic extensional structures of the Neuquén Basin, which were inverted also as a transfer zone during the Miocene compressive deformation that formed the Malargüe fold and thrust belt, and, in addition, it is located in the southern margin of a Neogene syn-orogenic basin. The analysis of vent center location and vent morphology is helpful to determine basaltic vent alignments within the Payún Matrú Volcanic Field and to infer the syn-eruptive stress field. This analysis shows that vent alignments are compatible with the present-day maximum horizontal stress, as measured by break-out of oil wells.

1. Introduction

Volcanic eruptions are frequently observed to form alignments, by means of the spatial distribution of monogenetic cones, polygenetic volcanoes, or fissural eruptions (Alaniz-Alvarez et al., 1998; Cole, 1990; Connor et al., 2000; Gudmundsson, 2000; Takada, 1994). The state of stress in the lithosphere at the time of volcanism has a remarkable effect on the distribution of volcanic centers and in the configuration of their plumbing system (Nakamura, 1977; Paulsen and Wilson, 2010; Takada, 1994) and therefore in the alignments of vents. In addition, the presence of pre-existing structures in the crust may serve as pathways for magma ascent, and therefore volcanic vents may be related to these crustal structures (Connor et al., 2000; Geyer and Martí, 2010; Petrinovic et al., 2006; Tibaldi et al., 2010).

In this contribution we will analyze the vent density distribution and vent alignments in the Payún Matrú Volcanic Field (PMVF). The PMVF is located within the Quaternary Payenia Basaltic Province (Polanski, 1954), one of the most significant back-arc basaltic provinces in the Andean back-arc of western Argentina. The volcanic eruptions in Payenia frequently form vent alignments which are thought to mimic the orientation of basement structures (Bermúdez and Delpino, 1989; Folguera et al., 2009; Llambías et al., 2010). The volcanic vents in the PMVF are distributed in an east–west fringe, and this distribution is peculiar in Payenia and different from the other volcanic fields of this basaltic province. The aim of this study is to examine the relationship between pre-existing crustal structures, the present-day stress field, and the volcanism in PMVF, in order to understand the relationships between basement structures and the stress field in the locus of the volcanic activity.

2. Geological setting

2.1. Payenia Basaltic Province

The Payenia Basaltic Province (33°30′ S–38° S) is located in the Andean back-arc of the northern segment of the Southern Volcanic Zone (Fig. 1). Its age is Pleistocene–Holocene, beginning its activity about 2 Ma (Espanon et al., 2014; Folguera et al., 2009; Germa et al., 2010; Gudnason et al., 2012; Kay et al., 2006; Quidelleur et al., 2009), being the largest Quaternary back-arc province of South America with an area of around 16,000 km^2 (Bermúdez et al., 1993; Folguera et al., 2009). This province is composed mainly of monogenetic alkaline basalts with an intraplate geochemical affinity, and with relatively scarce polygenetic volcanoes (Hernando et al., 2012; Kay et al., 2006), such as Nevado, Payún Matrú and Payún Liso (Fig. 1). The volcanism of Payenia develops mainly in the foreland region, while it is poorly

* Corresponding author. Tel.: +54 221 4215677.
E-mail address: ihernando@cig.museo.unlp.edu.ar (I.R. Hernando).

http://dx.doi.org/10.1016/j.tecto.2014.03.003
0040-1951/

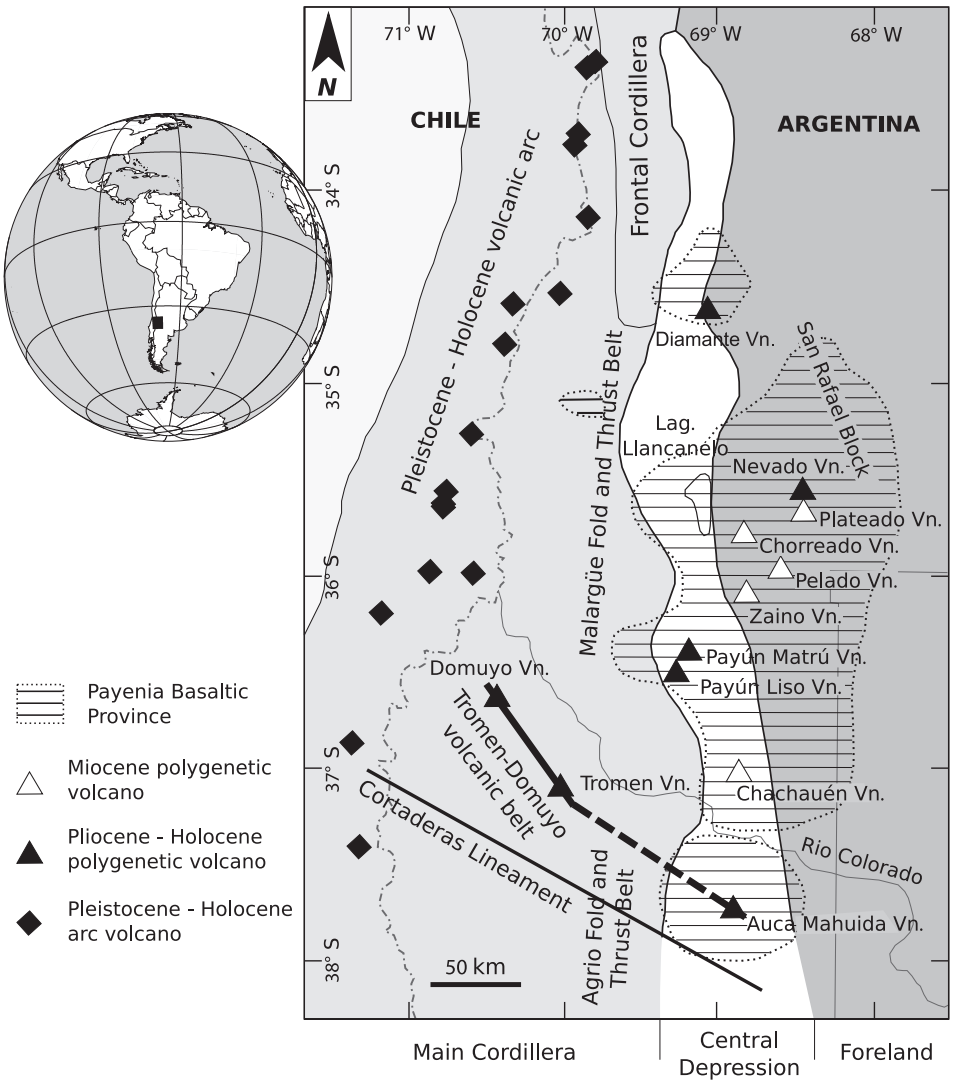

Fig. 1. Location of the Payenia Basaltic Province in the Andean back-arc, within the Southern Volcanic Zone. The Central Depression (Llambías et al., 2010) is located between the Main Cordillera and Frontal Cordillera (north of 34°30′ S).
Limits of the Central Depression and foreland are according to Llambías et al. (2010). Cortaderas lineament is drawn according to Ramos (1978), and Tromen–Domuyo volcanic belt is according to Llambías et al. (2010).

developed in the Orogenic Belt (Llambías et al., 2010). South of Auca Mahuida volcano (Fig. 1), the Central Depression and the Cenozoic basaltic back-arc volcanism are absent, limited by the Cortaderas lineament and the Tromen–Domuyo volcanic belt (Kay et al., 2006; Llambías et al., 2010; Ramos, 1978).

2.1.1. Overview of the Payún Matrú Volcanic Field

The Payún Matrú Volcanic Field is a Pleistocene–Holocene volcanic field located in southern Payenia (Germa et al., 2010; González Díaz, 1972; Gudnason et al., 2012; Llambías, 1966). It comprises two polygenetic (mostly trachytic in composition) volcanoes, Payún Matrú and Payún Liso, along with around 220 scoria cones and related basaltic lava flows (Fig. 2a). Payún Matrú is the biggest volcano in the field; it is a shield-shaped volcano with a summit caldera 8 km wide and a gentle slope (ca. 10°–15°).

The Payún Matrú volcano and scoria cones are distributed in an E–W oriented fringe about 15 km wide and 70 km long (Fig. 2a). The Payún Matrú caldera is located in the middle of this fringe, where no basalts occur. Thus, the distribution of monogenetic cones and related basaltic lava flows is divided into an eastern and a western basaltic field (Fig. 2a; Hernando et al., 2012). The presence of the Payún Matrú caldera and its associated ignimbrite sheet of upper Pleistocene age, the Portezuelo Ignimbrite, allowed the definition of three stages in the PMVF: a pre-caldera, a syn-caldera and a post-caldera stage (Fig. 2b; Hernando et al., 2012). The volcanic stratigraphic scheme is shown in Fig. 2b.

2.2. Pre-Payenia tectonic framework

The basement of Payenia is composed of Mesoproterozoic to Miocene sequences. The oldest units are exposed in the San Rafael Block (Criado Roque, 1972), which is composed of sedimentary, metamorphic and igneous rocks ranging from Mesoproterozoic to Triassic (Cingolani and Varela, 1999; Llambías et al., 1993). The Mesozoic units are represented by the infill of the Neuquén Basin, which is a huge extensional basin (32°–40° S) generated in the western margin of Gondwana by the Late Triassic to Lower Jurassic times (Franzese and Spalletti, 2001; Legarreta and Uliana, 1991; Vergani et al., 1995). A compressional tectonic regime active from the Late Cretaceous inverted the previous extensional structures (Vergani et al., 1995), and the basin evolved to a foreland retro-arc basin (Howell et al., 2005).

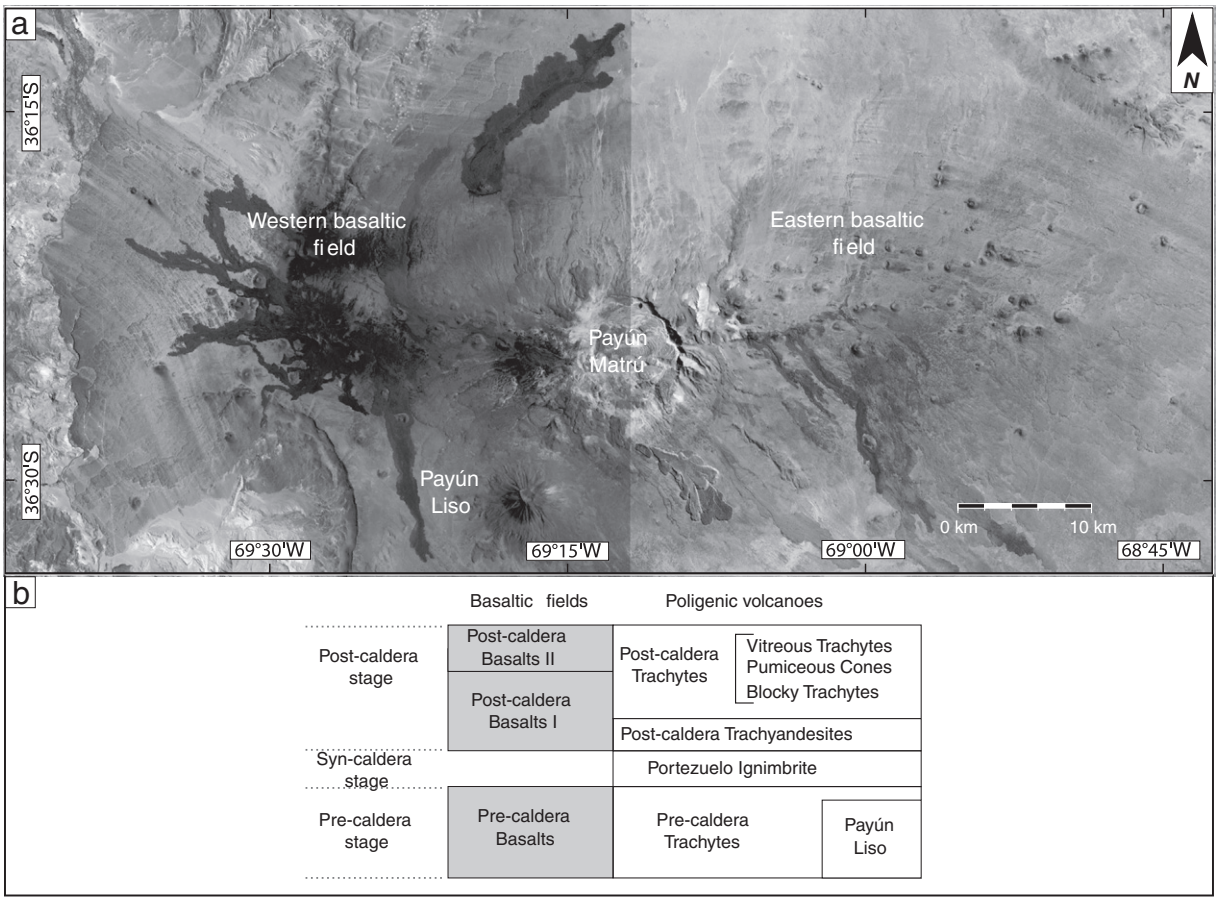

Fig. 2. a) LANDSAT 7 satellite image of the PMVF. b) Stratigraphic scheme of the PMVF. Modified from Hernando et al. (2012).

In the PMVF area, two Early Jurassic depocenters of the Neuquén Basin are present: the Palauco and Chacay Melehue half-grabens (Fig. 3; Manceda and Figueroa, 1995). The Palauco half-graben, interpreted on the basis of exploration wells, presents more than 1200 m of Jurassic sediments distributed in 1800 km^2, delimited by a major N–S fault along its western limit (Manceda and Figueroa, 1995). The Palauco half-graben was later inverted during the Cenozoic compressive regime, and their listric border faults were reactivated involving the basement (Manceda and Figueroa, 1995). The Chacay Melehue depocenter (Fig. 3) is located southwest of the Palauco half-graben, and it continues further south, with more than 2000 m of Jurassic sediments and a preserved area of 12,000 km^2 (Manceda and Figueroa, 1995). Both depocenters are laterally displaced (Fig. 3), which implies a Jurassic extensional transfer zone (Morley, 1995) between the active borders of these half-grabens, with a nearly E–W orientation.

In the Cenozoic Andean orogeny, the compressive regime led to the development of the Malargüe and Agrio fold and thrust belts, and the exhumation of the San Rafael Block (Fig. 1; Howell et al., 2005). The Agrio fold and thrust belt (36°–38° S) began in Late Cretaceous and it was later reactivated during the compressive regime of the Late Miocene (Zapata and Folguera, 2005). The main contractional deformation in the Malargüe fold and thrust belt occurred in the late Miocene (between 10.5 and 8 Ma, Giambiagi et al., 2008), and lasted until the Pliocene (Giambiagi et al., 2009). The Malargüe fold and thrust belt comprise low angle reverse faults with N–S and NNE trends (Fig. 4), and also high angle reverse faults with NW and NNW strikes (Giambiagi et al., 2009). The San Rafael Block is an asymmetric basement block uplifted in Late Miocene to Early Pliocene by high angle NNW–SSE and NNE–SSW reverse faulting in its eastern border (Fig. 4) (Folguera et al., 2009; Ramos and Kay, 2006; Sagripanti et al., 2012). At the PMVF latitude, the Neogene compression is displaced to the east (Fig. 4), which results in the uplifting of the San Rafael Block and implies a transfer zone of the Neogene deformation. This transfer zone is spatially coincident with the Jurassic accommodation zone between the Palauco and Chacay Melehue half-grabens. The PMVF is located in both these Jurassic and Neogene transfer zones.

Between the Malargüe fold and thrust belt and the San Rafael Block, there is a topographic low known as the Central Depression (Llambías et al., 2010), within which a foreland basin was developed in the vicinity of Laguna Llancanelo, i.e. the Malargüe Basin (Fig. 1; Silvestro et al., 2005). The beginning of this foreland basin could be in the Middle Miocene (ca. 16 ma ago) according to ages presented in Silvestro et al. (2005) and paleontological data of the Aisol Formation (Forasiepi et al., 2011; Soria, 1983), although most of its infill are Late Miocene–Pliocene syn-orogenic sediments and Pleistocene–Holocene post-orogenic sediments (Silvestro et al., 2005). The lowest area of the Central Depression, south of Río Salado (35° S, Figs. 1 and 4), presents an endorheic drainage towards the Laguna Llancanelo, and therefore this foreland basin has also been referred as the Llancanelo basin in Llambías et al. (2010). The thickness of the Pliocene–Quaternary sedimentary sequences in the Malargüe basin is highly variable but around 1000 m (Llambías et al., 2010; Ostera and Dapeña, 2003).

The Malargüe Basin disappears south of the Payún Matrú Volcanic Field, where the Pleistocene basalts overlie Cretaceous and Paleogene rocks of the Neuquén Basin and Miocene lava flows, in the vicinity of Chachauén and Auca Mahuida volcanoes (Fig. 1; Llambías et al., 2010; Rossello et al., 2002). The southern limit of the Malargüe basin is close to the PMVF latitude, since in the Salar El Cortaderal (~36° 40′ S and ~68°30′ W) Pleistocene basalts of Payenia cover Cretaceous–Paleocene sediments of the Malargüe Formation of the Neuquén Basin (Fig. 4).

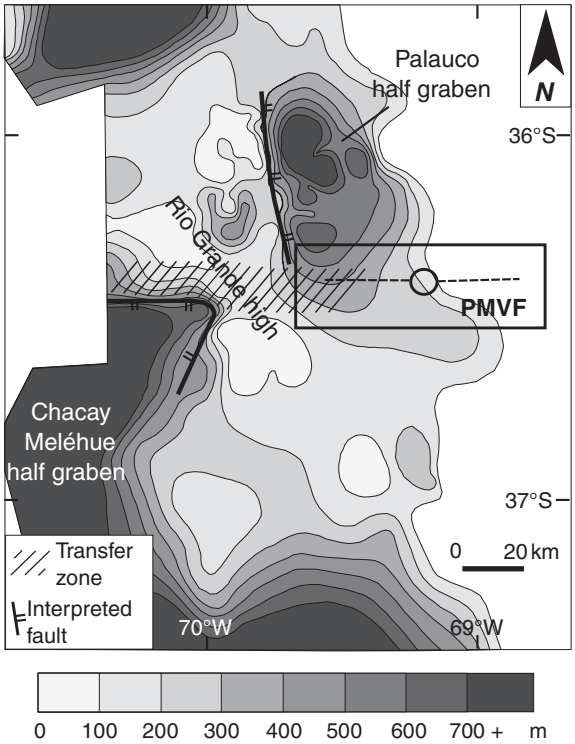

Fig. 3. Palinspastically restored isopach map of the Jurassic fill, based on well and surface data. The Jurassic infill represent syn-rift and post-rift sediments. The areas with lesser thickness and outside the depocenters correspond to post-rift sedimentation. Modified after Manceda and Figueroa (1995).

2.3. Spatial distribution of the volcanic activity in Payenia

Vent alignments in Payenia follow five main orientations (Fig. 4): the most important are NE–SW, NW–SE, NNW–SSE, and with less representation there are N–S and E–W alignments (Mazzarini et al., 2009). In the Northern segment of Payenia, the relatively monogenetic cones are associated with two NW–SE fault zones with sinistral strike-slip displacements, and also with minor E–W vent alignments (Fig. 4; Cortés and Sruoga, 1998). In the central zone of Payenia the volcanic eruptions above the San Rafael Block formed NW–SE vent alignments, reaching up to 60 km in longitude (Fig. 4; Bermúdez et al., 1993), and which were related to reactivation of Paleozoic faults of the volcanic basement (Llambías et al., 2010). In the northern zone of the Nevado Volcanic Field (~35° S), there is a NW fault system (Fig. 4) related to basaltic eruptions (Folguera et al., 2009). Vent alignments with E–W orientation and up to 10 km long are present near the Laguna Llancanelo (Fig. 4; Bermúdez and Delpino, 1989).

Basaltic vents in the Payún Matrú Volcanic Field (Fig. 4) are distributed along E–W and N 60° W fractures (Bermúdez and Delpino, 1989; Bermúdez et al., 1993; Mazzarini et al., 2009). A few Pleistocene lavas of Payenia were erupted within the Malargüe fold and thrust belt, near Río Salado and further south (Fig. 1; Llambías et al., 2010; Gudnason et al., 2012). The monogenetic cones in this region are controlled by N–S and also NW structures of the fold and thrust belt (Fig. 4; Llambías et al., 2010; Gudnason et al., 2012).

3. Vent distribution and alignments in PMVF

3.1. Volcanic vents as stress indicators

Vent alignments are common features both in arc/back-arc and intraplate settings. They frequently are the surface expression of almost planar vent systems in deep (Ancochea et al., 1996; Németh and Martin, 2007) and are strongly related with the syn-eruptive stress field. Hence, the presence and identification of vent alignments is important to infer the maximum horizontal stress present in a region at the time of volcanism, if the alignments are not influenced by pre-existing crustal structures. These vent alignments can be used as stress indicators in cases where vents are not affected by the presence of a polygenetic volcano or a magma chamber in the crust (Gudmundsson, 2006; Paulsen and Wilson, 2010). A magma chamber in the crust has the effect of deviate the regional stresses around it, although the influence of the magma chamber disappears at a relatively short distance from it (Gudmundsson, 2006). The fractures produced by the internal pressure of the magmatic chamber, or others fractures present in the country rock, tend to orientate perpendicular to the magma chamber wall, if the magma inside the chamber does not contain a high percentage of crystals and therefore do not acquire resistance. As indicated by analytical and numerical models, the influence of the magma chamber in the regional stress orientation reaches a distance away from the chamber of about the diameter of it, and further away the orientation of the stress field shows no deviations (Gudmundsson, 2006).

Vent alignments are common in the western and eastern basaltic fields of PMVF. The presence of Payún Matrú volcano (and also pre-existing crustal structures) may have influenced the orientations of vent alignments and fissural eruptions, and therefore it is important to consider their distance to the polygenetic volcano (Corazzato and Tibaldi, 2006). The Payún Matrú caldera is a strong evidence for the presence of a shallow magma chamber (Lipman, 2000; Parfitt and Wilson, 2008), at least during the syn- and post-caldera stages. It is assumed here that the diameter of the caldera is approximately equal to the diameter of the magma chamber, due to the recurrent geometry of reverse and normal faults formed during caldera collapse, which conform a relatively vertical annular zone around the chamber margins, as shows different analogous and numerical models (Acocella, 2007, and references therein; Gudmundsson, 2007a).

To identify vent alignments, it is important not only the center location of vents, but also the morphology of scoria cones, the presence of fissural ridges and/or fissural eruptions that lack the presence of a significant topographic relief (Paulsen and Wilson, 2010; Tibaldi, 1995). Elongated cones and fissural ridges, common in the basaltic fields, are reliable indicators of the stress field because they are the surface expression of the orientation of the feeder dyke (Paulsen and Wilson, 2010). The study of the vents is particularly important in cases where the erosion of the volcanic field has not been enough as to expose the sub-superficial feeder dykes, which are only observed in rare occasions (Galindo and Gudmundsson, 2012; Geshi et al., 2010).

3.2. Distribution and morphology of eruptive centers

The center location of basaltic and trachytic eruptions were mapped using a GIS software and LANDSAT 7 as well as Google Earth Pro images (license key JCPMM7BUX3EVPP3), and supported by field work (Fig. 5a). The monogenetic cones of the Pre-caldera Basalts unit were identified according to their partial cover by the Portezuelo Ignimbrite or, where the field control was not possible, according to their relatively advanced state of erosion or their previous identification in Llambías (1966). The basaltic cones of the Post-caldera Basalts I and II units were divided according to their lava flows (lava flows originated in the Post-caldera Basalts II cones cover those of the Post-caldera Basalts I), and also according to their better preservation in terms of the scarce vegetation cover. The field studies were carried out between ~69°30′ W and 69°00′ W (Fig. 5a), and therefore the majority of the monogenetic cones outside these limits could not be assigned precisely to a basaltic unit. Therefore, these cones were grouped in a fourth unit: the undifferentiated basalts (they correspond either to the Pre-caldera Basalts or the Post-caldera Basalts I units).

Since the diameter of the Payún Matrú caldera is about 8 km, the basaltic vents structurally influenced by its presence would be at a

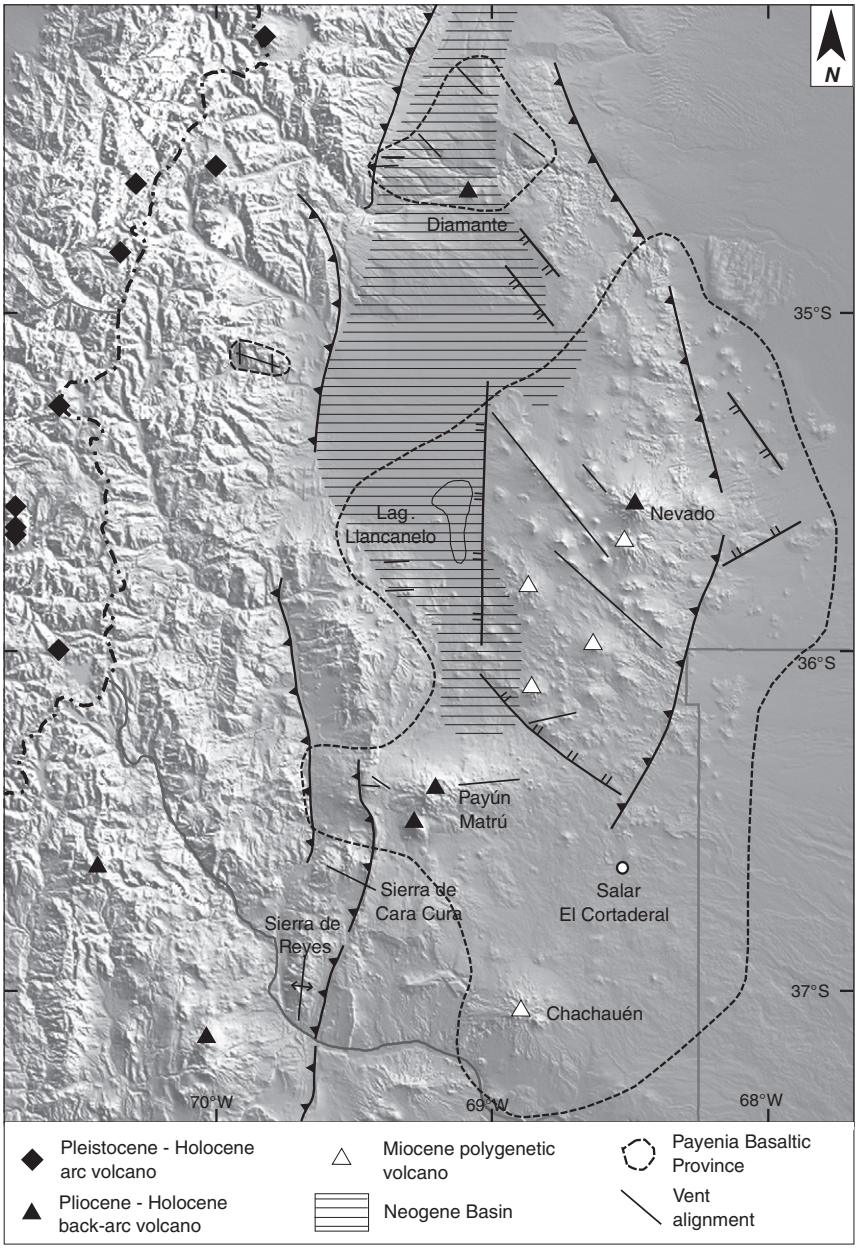

Fig. 4. DEM (SRTM; Rodríguez et al., 2005) showing the limits of the Neogene foreland basin (Llambías et al., 2010; Silvestro and Atencio, 2009; Silvestro et al., 2005), the main thrusts of the Miocene Malargüe fold and thrust belt (Guzmán et al., 2011; Sagripanti et al., 2012; Turienzo et al., 2010), main thrusts in the San Rafael Block (Folguera et al., 2009; Ramos and Folguera, 2011), Quaternary extensional faults (Folguera et al., 2009; Ramos and Folguera, 2011), and the main volcanic alignments in Payenia (Bermúdez and Delpino, 1989; Bermúdez et al., 1993; Cortés and Sruoga, 1998; Llambías et al., 2010; Mazzarini et al., 2009).

distance of around 8 km from the caldera margin. Most of the basaltic vents in PMVF are located outside this area of influence of the caldera, and therefore they can be used as stress indicators (Fig. 5a). Given the abundance of fissural eruptions and elongate cones or ridges, we consider more appropriate to determine vent alignments considering also the vent morphology rather than only the center location of each vent.

The vent density distribution was determined by means of a density map of the basaltic vents ("heat map" with points with a 3 km radius and a decay ratio of 0.1, Fig. 5b). In the density map (without the trachytic vents highly influenced by caldera structures) it is shown that the basaltic vents are concentrated in an east–west zone near the caldera, with a greater concentration in the western basaltic field (Fig. 5b). Further away from the caldera the vents are more dispersed and also, the vent density map shows higher concentrations with different orientations. Of the 223 identified vents in the PMVF, 122 are present in the western basaltic field, 98 are in the eastern basaltic field, and only 3 vents are located north of the caldera. In the eastern basaltic field, the vents in its eastern sector present higher densities with NW–SE orientations, similar to the alignments observed in the Nevado Volcanic Field and faults present in the San Rafael Block (Figs. 4 and 5b). In the western basaltic field, the vents in its western sector have a density concentration with NE–SW orientation (Fig. 5b), similar to the orientation of some Neuquén basin structures and dikes and asphaltite veins present in Sierra de Cara Cura and Sierra de Reyes (Cobbold et al., 2011).

The morphology of craters and the bases of scoria cones (which may be obliterated by later lavas in some cases), the ridges of fissural ridges and the traces of the fissural eruptions were mapped (Fig. 6). Alignments in the basaltic fields were identified by means of the center location of vents, vent morphology (crater and basal shapes where it was possible) and also fissural eruptions that lack a significant topographic expression (Fig. 7). The breaching direction of scoria cones can be

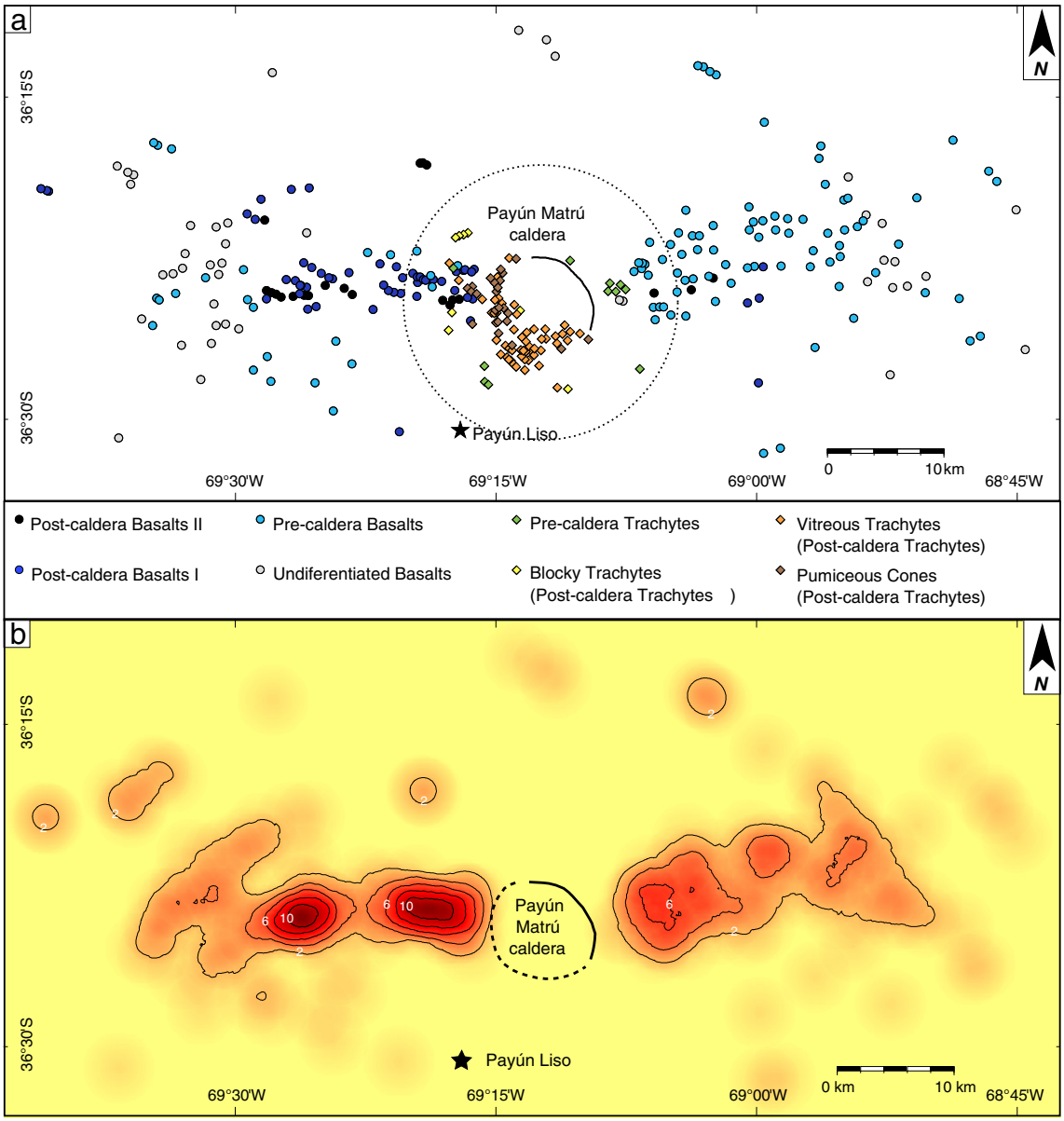

Fig. 5. a) Map with the center location of volcanic vents, showing the general east–west distribution of vents in the PMVF, and the area of influence of Payún Matrú caldera (point line circle). b) Density map of the basaltic vents only, which shows in red the zones of highest vent density in the volcanic field.

used to infer fissures, when the topography is sub-horizontal (Corazzato and Tibaldi, 2006; Tibaldi, 1995). Breaching in cones is common in the PMVF, but since it is observed that in most cases the breaching is controlled by topography, it was not used to determine alignments.

The morphology of crater and bases of scoria cones varies from circular to highly elongated (Fig. 6). Besides, the fissural ridges and other scoria and spatter deposits indicate the strike of the fissure (Fig. 7). This is observed, e.g. in a 1650 m long fissural eruption in the western basaltic field, in which there are seven circular spatter accumulations a few meters in diameter, two small cones (less than 100 m in diameter), and one scoria cone, all of which are aligned in a WNW direction (Fig. 7a,b). Other example is a fissural eruption near the caldera, in the eastern basaltic field, in the so-called La Carbonilla fault (Fig. 7c; González Díaz, 1972; Llambías et al., 2010).

In the Payún Matrú volcano, the base of the pumiceous cones were mapped as were the scoria cones but, in contrast to their basaltic equivalent, they usually lack a crater and may have an elongated ridge instead (Fig. 6). Alignments in the Payún Matrú caldera area where no scoria cones are present were defined using the morphology of pumiceous cones and the locus of lava domes and lava flow vents.

3.3. Analysis of vent alignments in the PMVF

Where no fissural eruptions are present, or when there are no elongated cones, there must be three or more adjacent cones to define an alignment. Less than three cones can define an alignment if there is a clearly elongated vent and/or fissural ridges or eruptions, since these indicate the trace of the feeder dyke (Paulsen and Wilson, 2010). The alignments defined in the basaltic fields and the Payún Matrú volcano were divided qualitatively in two types, A and B, according to their degree of confidence. Type A alignments are those that present a clear fissural eruption, or fissural ridges plus three or more vents, or 5 or more vents separated by hundreds of meters. Type B alignments are those that present fissural ridges plus one or two scoria cones, or three or four vents with neither evident fissural eruptions nor fissural ridges. The longitude of the alignments defined span between 738 m and 9480 m (with a mean longitude of 3421 m), and the longest ones

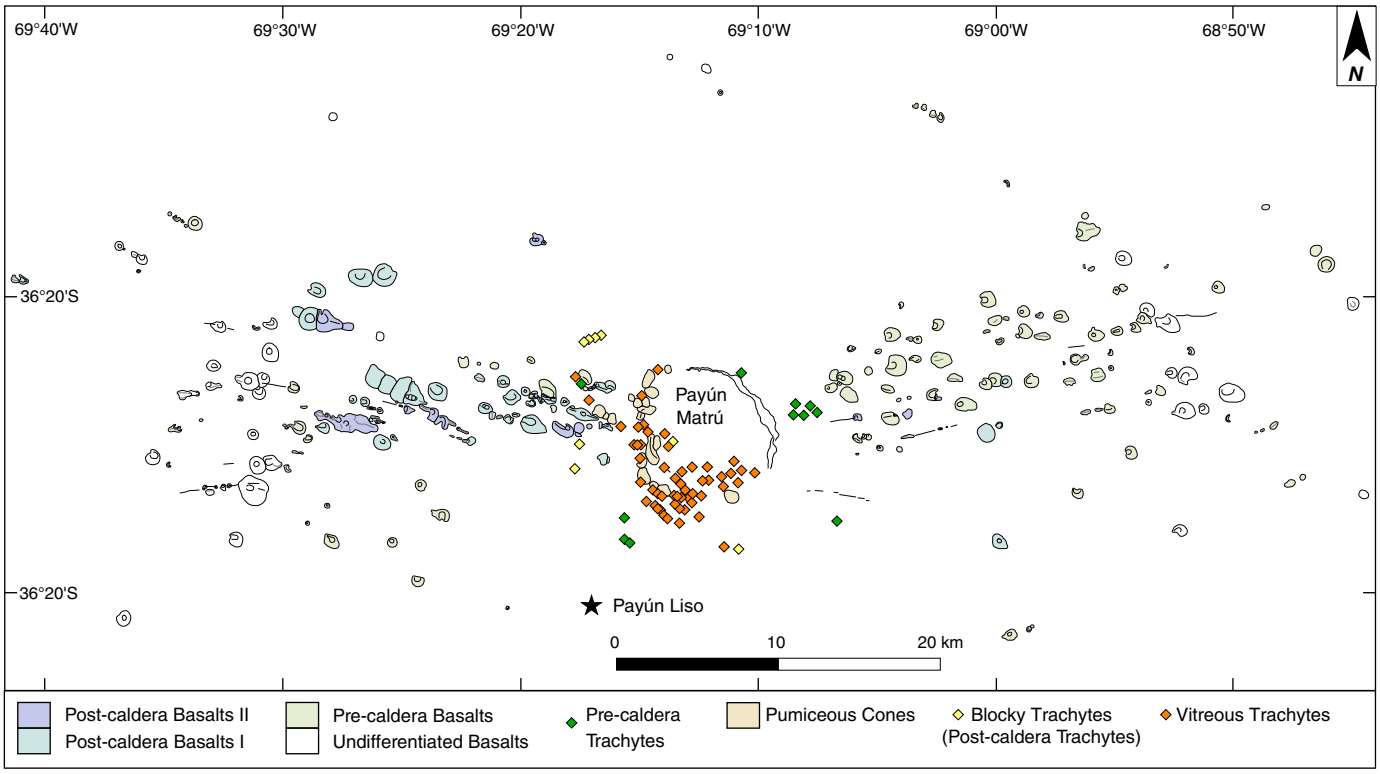

Fig. 6. Map showing the vent morphology in the eastern and western basaltic fields. The base and crater of scoria cones are drawn, as well as the trace of fissural eruptions with minimal topographic expression and the ridges of elongated cones or fissure ridges. The vent location of Payún Matrú trachytic lavas is also shown.

are present in the eastern basaltic field. Fig. 8 shows the alignments defined based on location and morphology of basaltic and trachytic vents.

Twenty five alignments formed by basaltic eruptions were identified in the eastern basaltic field, while 30 were identified in the western one. Of each alignment, the longitude, azimuth and type were determined, along with the number of vents and the presence of fissural ridge or a fissural eruption (Table 1). Fig. 9 shows the rose diagrams for all the alignments identified in the eastern and western basaltic fields, sepa-

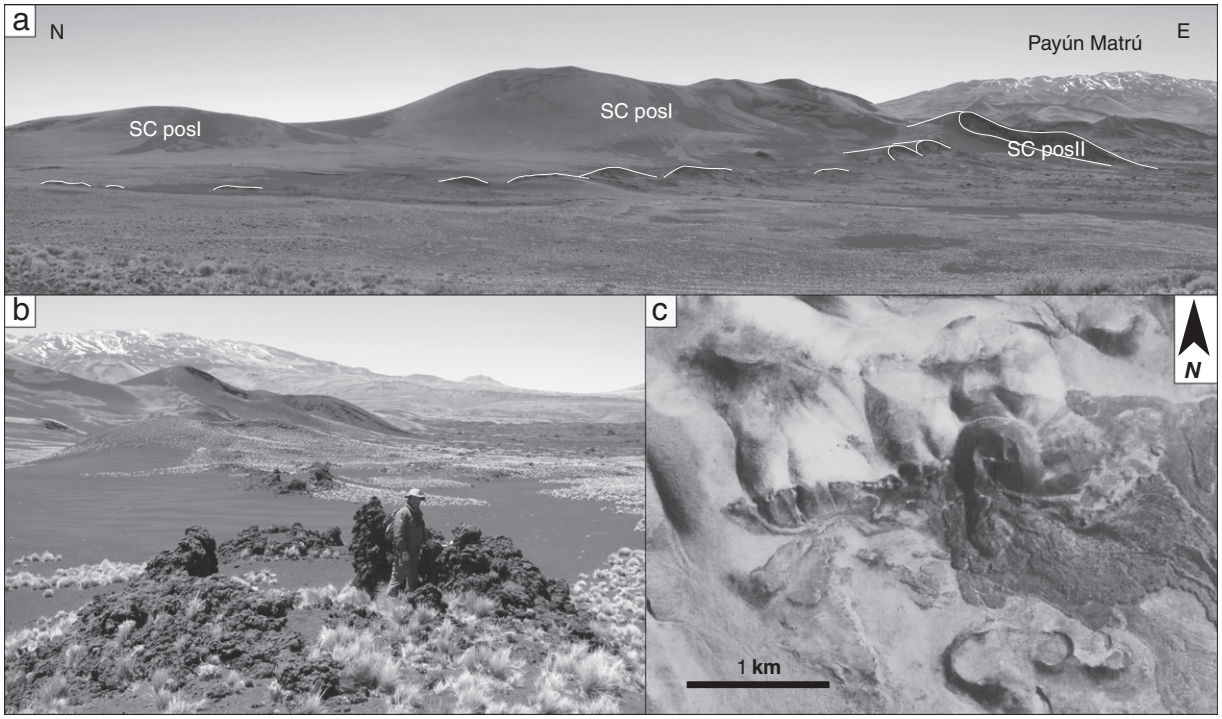

Fig. 7. Photographs of basaltic fissural eruptions. a and b) Seven spatter accumulations as in photo b, two small cinder cones and one well developed scoria cone, with a NW–SE orientation, in the western basaltic field (Post-caldera Basalts II unit). SC posI: post-caldera basalt I scoria cone; SC posII: post-caldera basalt II scoria cone. c) Fissural eruption in the La Carbonilla Fault, in the eastern basaltic field.

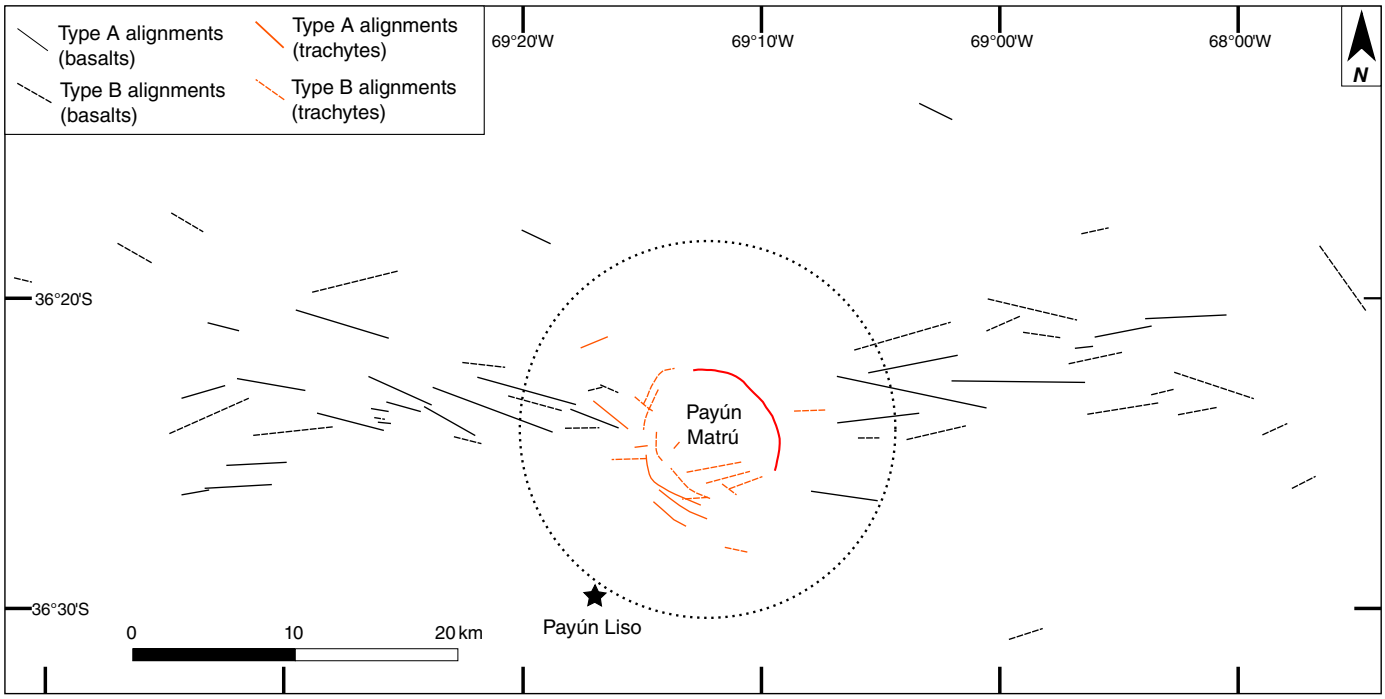

Fig. 8. Vent alignment map which results from the analysis of vent location and morphology.

rately. Although both fields show near E–W orientations, there is clearly a difference between them.

The orientations of all the alignments present in the eastern basaltic field have a mean azimuth of N 87°, although the direction with higher frequency is in the range of N 71°–80° (Fig. 9b). Other directions with lesser representation are approximately E–W (between N 80° and N 100°), and scarce NW–SE alignments (Fig. 9b). In regards to the type A alignments of the eastern basaltic field, the most frequent directions are in the N 81°–90° range (with a mean value of 91°), while the most frequent type B alignments are have an azimuth between N 71° and N 80°, with a mean direction of 84° (Fig. 9d). The only alignment with a NW–SE direction in this field is the most farther away from the caldera (Fig. 8). Its orientation is the same as those observed in the Nevado Volcanic Field, which presents NW–SE vent alignments and is located above the San Rafael Block. The location of this alignment in the PMVF suggests that the most eastern portion of the volcanic field is controlled by the San Rafael Block structure.

In the western basaltic field, the preferred orientations of vent alignments have slightly different orientations than in the eastern field (Fig. 9a). The mean azimuth of all alignments is N 99°. The directions with higher frequency are ESE (azimuth between N 101° and N 110°) and with lesser representation are near E–W directions (between N 80° and N 90°, Fig. 9a). There are some differences in the orientations of type A and type B alignments (the ENE and NW directions are more important in the type B alignments), although the prevalent orientations are the same as described above (Fig. 9c).

In order to compare the vent alignments of areas partly or completely inside the caldera with areas outside of it, rose diagrams were performed, showing no significant differences (Fig. 9d,e). Of the twenty-five alignments defined in the eastern basaltic field, only six are fully or partly within the area of influence of the Payún Matrú caldera, according to the considerations of Gudmundsson (2006). In the eastern basaltic field, the rose diagrams of alignments within and outside of the caldera influence show the same mean direction (N 86° and N 88°) and the same most frequent range (between N 71° and N 80°) (Fig. 9f), although the E–W direction is more important in the alignments within the area of influence of the caldera. As in the previous case, most of the vent alignments in the western basaltic field lie outside the zone of Payún Matrú caldera influence (only seven of thirty within this area), and they do not show major differences with the alignments farther from the caldera. The mean direction is the same in both cases (N 99° and N 102°), but the frequencies vary slightly (Fig. 9e). Nevertheless, in the proximity of the caldera the vents are concentrated in a narrower zone than in areas away from it (Fig. 5a,b). Thus, the presence of Payún Matrú volcano and its caldera seems to have an influence on the location and density of vents, but no significant influence is observed in the orientation of the vent alignments.

The differences observed in the orientations of alignments in the eastern and western basaltic fields are not only spatial, but also temporal. This is because in the eastern basaltic field the majority of the alignments defined are those formed by pre-caldera basalt vents, while in the western basaltic field the alignments formed by post-caldera basalt I and II vents predominate.

In the Payún Matrú caldera, alignments of trachytic domes, pumiceous cones and vents of trachytic lava flows are observed (Fig. 8). These alignments are distributed in the SE to N margin of the caldera, in an annular zone that widens in the southern margin (Fig. 8). In contrast with the basaltic fields, the orientation of the trachytic vent alignments is highly variable, in accordance with the annular structure of the caldera. In the slope of Payún Matrú, some trachytic and basaltic eruptions share the same orientation. This can be observed in the western flank of the volcano, with two lava flows and three pumiceous cones aligned NW–SE (Figs. 5a and 8). In the eastern slope of Payún Matrú, trachytic domes are concentrated near the caldera margin with an E–W orientation, similar to adjacent basaltic fissural eruptions (Fig. 5a).

3.4. Stress field in PMVF as inferred by vent alignments

Vent alignments may represent new fractures produced by hydraulic opening related to magma overpressure and/or incremental deformation (oriented according to the stress field in the upper crust present at the time of volcanism, i.e. perpendicular to the minimal compressive stress sigma 3 and parallel with the maximum compressive

Table 1
Vent alignments defined within the Payún Matrú Volcanic Field.

Alignment ID	Azimuth (°)	Longitude (m)	# Vents	Fissural ridges	Fissural eruptions	Type	Influenced by caldera	Basaltic field
1	104	1067	3	No	No	B	No	Western
2	120	2387	3	No	No	B	No	Western
3	121	2239	3	No	No	B	No	Western
4	107	5990	4	Yes	No	A	No	Western
5	104	1946	1	No	Yes	A	No	Western
6	74	2757	3	Yes	No	A	No	Western
7	100	4252	4	No	Yes	A	No	Western
8	66	5351	4	No	No	B	No	Western
9	87	3694	3	No	Yes	A	No	Western
10	87	4123	3	Yes	Yes	A	No	Western
11	80	1672	0	No	Yes	A	No	Western
12	84	4989	3	No	No	B	No	Western
13	105	4231	5	Yes	No	A	No	Western
14	96	738	3	Yes	No	A	No	Western
15	99	591	0	Yes	No	B	No	Western
16	106	2153	1	Yes	Yes	A	No	Western
17	114	4254	5	Yes	No	A	No	Western
18	100	1036	3	Yes	No	A	No	Western
19	120	3593	3	Yes	No	A	No	Western
20	104	1687	1	Yes	No	B	No	Western
21	111	3155	3	Yes	No	A	Yes	Western
22	76	837	2	Yes	No	B	Yes	Western
23	114	1148	2	Yes	No	B	Yes	Western
24	106	6316	10	No	No	A	Yes	Western
25	105	3502	3	No	No	B	Yes	Western
26	89	2064	3	No	No	B	Yes	Western
27	110	7921	6	No	No	A	Yes	Western
28	96	2611	3	No	No	B	No	Western
29	76	5432	3	No	No	B	No	Western
30	115	1921	3	No	Yes	A	No	Western
31	98	4127	0	No	Yes	A	Yes	Eastern
32	83	5079	4	No	Yes	A	Yes	Eastern
33	102	9480	7	Yes	No	A	Yes	Eastern
34	77	3723	1	Yes	No	B	No	Eastern
35	90	1256	3	No	No	B	Yes	Eastern
36	72	2136	2	Yes	No	B	No	Eastern
37	91	8265	6	Yes	No	A	No	Eastern
38	79	5618	4	Yes	No	A	Yes	Eastern
39	74	6194	3	No	No	B	Yes	Eastern
40	103	5654	4	No	No	B	No	Eastern
41	66	2198	3	No	No	B	No	Eastern
42	84	1059	0	No	Yes	A	No	Eastern
43	81	4496	2	Yes	No	B	No	Eastern
44	79	3325	2	Yes	No	B	No	Eastern
45	63	1580	2	Yes	No	B	No	Eastern
46	65	1627	1	Yes	No	B	No	Eastern
47	76	1458	1	Yes	No	B	No	Eastern
48	79	2471	2	Yes	No	B	No	Eastern
49	87	5007	3	No	Yes	A	No	Eastern
50	79	3546	3	Yes	No	A	No	Eastern
51	144	4887	3	No	No	B	No	Eastern
52	78	1664	1	Yes	No	B	No	Eastern
53	116	2218	4	Yes	No	A	No	Eastern
54	108	5161	3	No	No	B	No	Eastern
55	98	2264	2	Yes	No	B	No	Eastern

stress sigma 1; Gudmundsson, 2011) with or without the influence of pre-existing crustal anisotropies. These new fractures usually develop from minor weaknesses in the crust, such as cooling joins (Gudmundsson, 2011). Although the general E–W vent distribution of PMVF seems to be controlled by crustal structures, the strike of vent alignments within the volcanic field suggests that they respond mostly to the expected stress field present at the moment of volcanism (also with minor basement structures influence). The stress field is expected to be controlled basically by two type of forces: the plate-boundary forces (maximum horizontal stress with a mean azimuth of N 80°) and the forces exerted by the thickened crust in the Main Cordillera, with an E–W oriented maximum horizontal stress (Guzmán et al., 2007; Meijer, 1997). We will first consider the vent alignments as representing the orientation of the stress field coeval with the volcanic activity, with no influence of pre-existing crustal structures, in order to compare this inferred stress orientation with the actual present-day orientation of the maximum horizontal stress (sigma 1 or sigma 2).

The observed differences in the orientations of basaltic vent alignments between the eastern and the western basaltic fields, suggest that there may have been only a slight difference in the orientation of the maximum horizontal stress during the Pleistocene–Holocene evolution of the PMVF. The eastern basaltic field presents some conjugate alignments, with acute angles of around 30° and the bisector in an E–W direction (Fig. 8). The acute angle is too small to represent conjugate shear faults with a maximum horizontal stress oriented E–W, which should be around 60° according to the Anderson's law. In addition, this configuration of conjugate faults and stress should produce slip in the fault planes, which is not observed. In addition to pure shear and pure tension fractures, the fractures can be also hybrid, in which both shear and aperture occur (Ramsey and Chester, 2004).

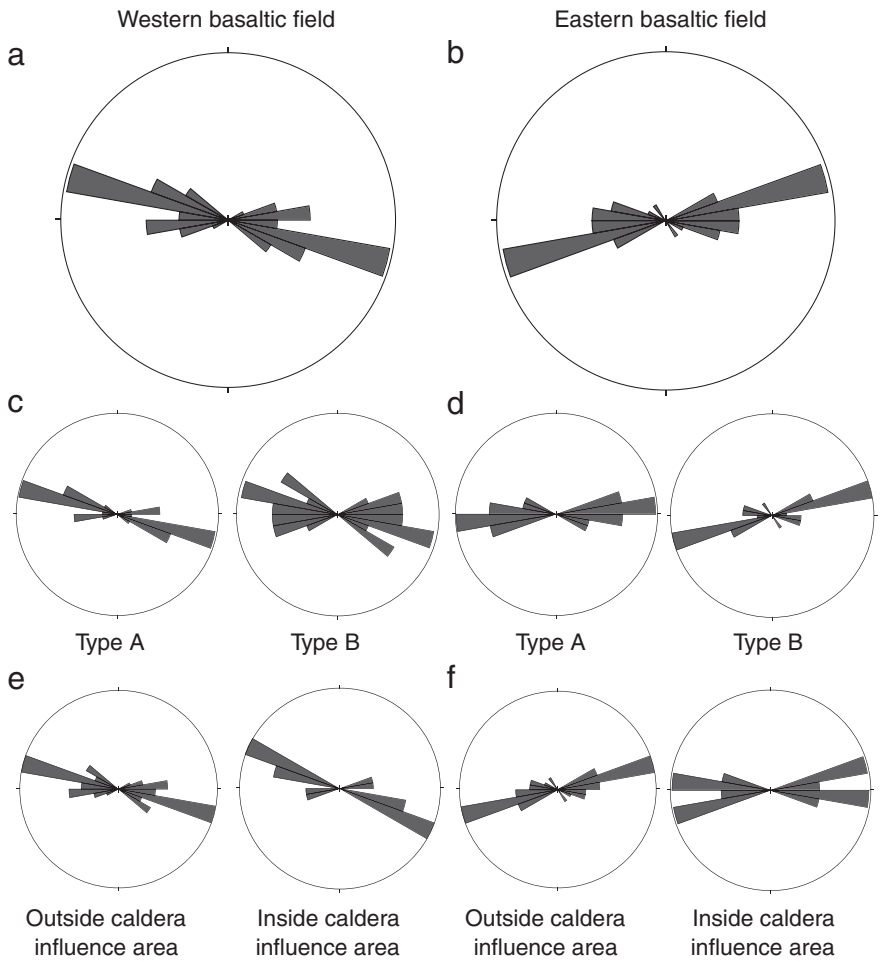

Fig. 9. Rose diagrams of the eastern and western basaltic field alignments, with a 10° interval. Determined with the Stereonet 8 software, Allmendinger et al. (2012).

Hybrid fractures can form conjugate fractures with a lesser acute angle than in the case of shear fractures, and they are formed under a mixed stress field with both compression and extension (Ramsey and Chester, 2004). As in shear fractures, the orientation of the maximum horizontal stress in hybrid fractures is coincident with the bisector of the acute angle between the conjugate fractures (Ramsey and Chester, 2004), which is E–W in the case of the eastern basaltic field. In addition to the hybrid fractures, the E–W alignments may represent purely tensional fractures, formed parallel to the maximum horizontal stress. Thus, the orientation of the basaltic vent alignments observed in the eastern basaltic field can be explained by means of an E–W maximum horizontal stress (predominating in the pre-caldera stage), which would produce the ENE–WSW and ESE–WNW conjugated hybrid fractures and the E–W tensional fractures.

In contrast to the eastern basaltic field, conjugated fractures are not observed in the western basaltic field (Fig. 8). The ESE preferred orientation of the vent alignments suggest a maximum horizontal stress in the same direction and the presence of tensional fractures (N 100°–110°), for the post-caldera stage of PMVF.

4. Discussion

4.1. Vent density distribution of the PMVF

The high density of vents in a relatively wide zone with an E–W orientation observed in the PMVF is not repeated anywhere else within Payenia, although some east–west vent alignments are observed in central and northern Payenia (Fig. 5). Since crustal structures and the stress field play a significant role in magma transport and storage, the difference in the distribution of volcanic vents in Payenia may be related to differences in basement structures and to the Quaternary tectonic activity.

The use of pre-existing or active structures for the ascent of magma is widely recorded around the world, and there are examples in different geodynamic settings; such is the case of Iceland, where dyke swarms are found in transform faults (Gudmundsson, 1995, 2007b). There are several features which suggest that the overall vent distribution in the PMVF is influenced by crustal anisotropies. First, the PMVF is located in a nearly E–W transfer zone that connect the southern limit of the uplifted San Rafael Block with the front of the Malargüe fold and thrust belt (Sagripanti et al., 2012), i.e. the Miocene deformation front north of the volcanic field is within the foreland region, and south of PMVF is in the Main Cordillera (Fig. 10). Second, the Neogene–Quaternary syn- and post-orogenic fill is significantly thick north of the PMVF in the Malargüe basin (around 1000 m of sediments, Ostera and Dapeña, 2003), while it disappears south of the PMVF (Figs. 4 and 10). Third, the Payún Matrú Volcanic Field is located in the southern margin of the Jurassic Palauco half-graben, and the western limit of the volcanic field is coincident with the western margin of the depocenter and a near E–W Jurassic transfer zone (Fig. 3). The E–W orientation of structures is not unusual in the Neuquén Basin, and this direction appears in other important basin structures, such as the Huincul high (Pángaro et al., 2009; Vergani et al., 1995).

The location of the PMVF near or within the southern border of the Neogene–Quaternary basin along with its location near the southern border of the Jurassic Palauco half-graben, mostly over the transfer

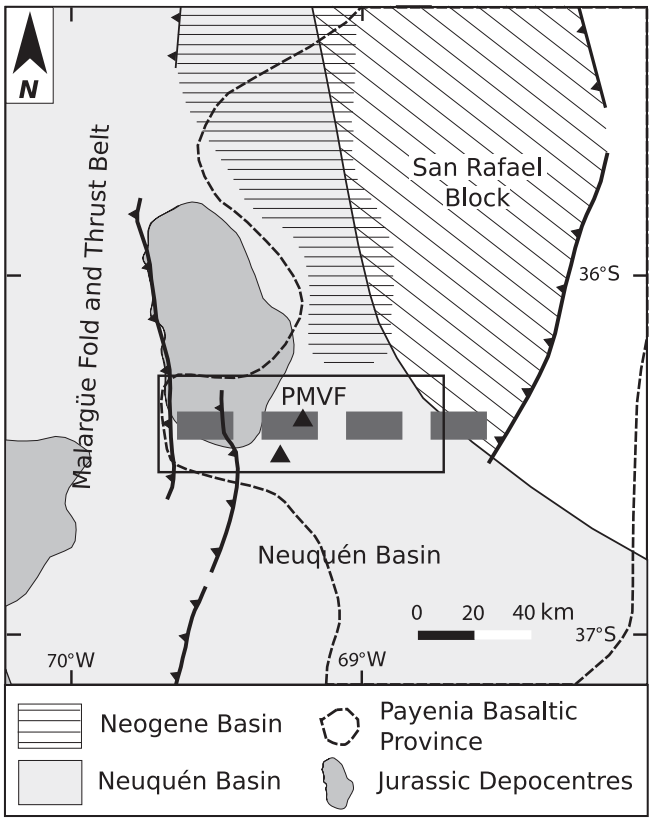

Fig. 10. Location of the PMVF within Payenia, in the southern border of the Neogene basin, in a transfer zone of the Miocene deformation and also in the southern border of the Jurassic Depocenter.

zone between the Jurassic syn-rift depocenters, suggests that this zone between the two half-grabens also controlled the southern limit of the Neogene foreland basin. In addition, the Jurassic transfer zone seems to have influenced the Miocene deformation, being the Jurassic and Miocene transfer zones at similar latitudes. Therefore, the overall east–west distribution of the volcanic field may be a reflection of the pre-existing crustal structures, which also controlled the deposition of the sedimentary sequences, at least since Jurassic times.

In the western zone of the western basaltic field, the basaltic vent density map shows a greater concentration of vents forming an NE–SW alignment (Fig. 5b). This orientation is similar to post-Pliocene dykes and asphaltite veins present in Sierra de Cara Cura and Sierra de Reyes, south-west from Payún Matrú (Fig. 4, dykes and veins not shown, Cobbold et al., 2011). Near the Sierra de Cara Cura these asphaltite veins are oriented NNE, while in Sierra de Reyes and south of it, the asphaltite veins present a NE orientation (Cobbold et al., 2011). In the eastern zone of the eastern basaltic field, the highest vent densities form NW–SE alignments (Fig. 5b), similar to vent alignments in the Nevado Volcanic Field and internal structures of the San Rafael Block. This distribution strongly suggests the control of pre-existing basement faults on the Quaternary PMVF volcanism.

The orientation of basaltic vent alignments do not seem to be affected by the presence of the Payún Matrú caldera, although a greater density of vents is observed in its vicinity (Fig. 5). The expected influence of Payún Matrú and its magma chamber/s in the distribution of basaltic volcanism would be to orientate the feeder dikes perpendicular to the chamber wall (Gudmundsson, 2006). The lack of influence of the Payún Matrú caldera in the orientation of vent alignments in its proximity could be due to the particular configuration of the eruptive centers. Since Payún Matrú is located in the middle of an E–W zone with maximum concentration of basaltic vents, and the general trend of basaltic vent alignments is ~E–W, then the orientation of fractures due to regional stresses and the orientation of fractures due to the caldera influence, coincide. Therefore, the presence of the polygenetic volcano does not seem to have an effect on vent alignment orientations, but it does have an influence increasing the basaltic vent density around it.

4.2. Vent alignments within the PMVF

The inferred maximum horizontal stress direction, as deduced by basaltic vent alignments alone, and without considering the influence of previous structures, would have a near E–W orientation. In the eastern basaltic field, where Pre-caldera Basalts vents predominate (Fig. 5), the maximum horizontal stress suggested is oriented E–W. A slight change is suggested in the western basaltic field, where Post-caldera Basalts I and II vents predominate over those of the pre-caldera stage. Here, the maximum horizontal stress is inferred to be ESE (azimuth N 100°–110°).

The inferred orientation of the maximum horizontal stress is consistent with the present state of stress in the PMVF region. The current horizontal stress field in the Neuquén Basin has been measured by breakout of oil wells (Guzmán et al., 2007, 2011). The preferred maximum horizontal stress orientation in the whole basin is N 89°, although there are differences south and north of Río Colorado (Fig. 1). North of Río Colorado the maximum horizontal stress has an ESE trend, with a mean azimuth of N 100° (Guzmán et al., 2007). These stress orientations are consistent with the expected stress field in the Andean foreland.

Although the general vent concentration in PMVF in an east–west zone seems to be controlled by crust anisotropies, the orientation of most of the vent alignments within the volcanic field suggest that these may respond also to the near-surface stress field. The ESE trend of the maximum horizontal stress suggested by the post-caldera vent alignments in PMVF matches the present-day measured stress field and also it is consistent with the expected stress field acting on the western margin of South America. The slight difference in the mean azimuth of pre-caldera vent alignments would suggest that the recent horizontal stress field in the Andean foreland could be responsible for the vent alignments in the early stage of the PMVF. Nevertheless, a few vent alignments in the margins of the volcanic field present an orientation clearly different of the expected according to the stress field (Fig. 8), such as the alignments that mimic the orientation of NW–SE structures within the San Rafael Block in the eastern basaltic field.

Considering the present-day stress field and the abundance of volcanic activity in a narrow east–west zone, the E–W crustal anisotropy that controls the locus of the volcanism in PMVF would be a suitable structure for magma ascent. While this crustal anisotropy controls the general vent density distribution of the PMVF, the nearly E–W present-day maximum horizontal stress seems to influence the strike of vent alignments within the volcanic field.

5. Conclusions

The overall E–W vent density distribution in PMVF is controlled by pre-existing crustal structures as evidenced by: i — the location of the volcanic field in the southern limit of Jurassic syn-rifts deposits, and also in a transfer zone within depocenters, which is nearly E–W; ii — the southern border of the Neogene basin is not determined precisely, but it is close to the location of the PMVF and may be also influenced by Jurassic structures; iii — the Miocene thrusts present a transfer zone at the latitude of the PMVF, being the thrust front south of PMVF in the eastern margin of the Main Cordillera, and north of PMVF in the eastern margin of the San Rafael Block in the foreland; iv — the most eastern basaltic vents are clearly distributed following the structures present in the San Rafael Block; and v — the most western basaltic vents in PMVF present the same orientation as dykes, asphaltite veins and other structures present in the Neuquén Basin.

Vent alignments within the PMVF were determined for the eastern and western basaltic fields, and the trend of these alignments is

coincident with the present-day measures of the maximum horizontal stress. Thus, crustal anisotropies have a significant influence on the general vent distribution of the PMVF, while the stress field in the most upper crust would control the orientation of most of the vent alignments within the volcanic field.

Acknowledgments

This work was supported by the Universidad Nacional de La Plata grants [N547, N620] to Eduardo J. Llambías and a Consejo Nacional de Investigaciones Científicas y Técnicas grant [PIP 112-200801-00119] to Ana María Sato. We would like to thank the staff of Recursos Naturales Renovables of Malargüe, Argentina, for all their support in the field works, and also Ariel Schiuma, Lucas Oliva, Matías Galina, Gerardo Páez and Federico González Soto for their help in the field. Thanks to Alfredo Benialgo for helping with the satellite images. Reviews by A. Gudmundsson and V. A. Ramos helped to improve the original manuscript.

References

Acocella, A., 2007. Understanding caldera structure and development: an overview of analogue models compared to natural calderas. Earth Sci. Rev. 85, 125–160.

Alaniz-Alvarez, S.A., Nieto-Samaniego, A.F., Ferrari, L., 1998. Effect of strain rate in the distribution of monogenic and polygenic volcanism in the Transmexican volcanic belt. Geology 26 (7), 591–594.

Allmendinger, R.W., Cardozo, N., Fisher, D.M., 2012. Structural Geology Algorithms, Vectors and Tensors. Cambridge University Press, Cambridge.

Ancochea, E., Brändle, J.L., Cubas, C.R., Hernán, F., Huertas, M.J., 1996. Volcanic complexes in the eastern ridge of the Canary Islands: the Miocene activity of the island of Fuerteventura. J. Volcanol. Geotherm. Res. 70, 183–204.

Bermúdez, A., Delpino, D., 1989. La provincia basáltica andino cuyana. Rev. Asoc. Geol. Argent. 44, 35–55.

Bermúdez, A., Delpino, D., Frey, F., Saal, A., 1993. Los basaltos de retroarco extraandinos. In: Ramos, V.A. (Ed.), Geología y Recursos Naturales de Mendoza, 12° Congreso Geológico Argentino and 2° Congreso de Exploración de Hidrocarburos, Relatorio. Asociación Geológica Argentina, Buenos Aires, pp. 161–172.

Cingolani, C.A., Varela, R., 1999. The San Rafael Block, Mendoza (Argentina): Rb–Sr isotopic age of basement rocks. South American Symposium on Isotope Geology, 2, Anales. Servicio Geológico Minero Argentino, 34, pp. 23–26. Servicio Geológico Minero Argentino, Buenos Aires.

Cobbold, P.R., Ruffet, G., Leith, L., Løseth, H., Rodrigues, N., Galland, O., Leanza, H.A., 2011. Combustible sólidos (asfaltita) de la provincia del Neuquén. 18° Congreso Geológico Argentino, Relatorio, Neuqúen, pp. 689–695.

Cole, J.W., 1990. Structural control and origin of volcanism in the Taupo volcanic zone, New Zealand. Bull. Volcanol. 52, 445–459.

Connor, C.B., Stamatakos, J.A., Ferril, D.A., Hill, B.E., Ofoegbu, G.I., Conway, M., Sagar, B., Trapp, J., 2000. Geologic factors controlling patterns of small-volume basaltic volcanism: application to a volcanic hazards assessment at Yucca Mountain, Nevada. J. Geophys. Res. 105 (1), 417–432.

Corazzato, C., Tibaldi, A., 2006. Fracture control on type, morphology and distribution of parasitic volcanic cones: an example from Mt. Etna, Italy. J. Volcanol. Geotherm. Res. 158, 177–194.

Cortés, J.M., Sruoga, P., 1998. Zonas de fractura cuaternarias y volcanismo asociado en el piedemonte de la Cordillera Frontal (34°10 S), Argentina. 10° Congreso Latinoamericano de Geología and 6° Congreso Nacional de Geología Económica. Actas, 2, pp. 116–121.

Criado Roque, P., 1972. El Bloque de San Rafael. In: Leanza, A.F. (Ed.), Geología Regional Argentina. Academia Nacional de Ciencias, Córdoba, pp. 283–295.

Espanon, V.R., Honda, M., Chivas, A.R., 2014. Cosmogenic ^{3}He and ^{21}Ne surface exposure dating of young basalts from Southern Mendoza, Argentina. Quat. Geochronol. 19, 76–86.

Folguera, A., Naranjo, J.A., Orihashi, Y., Sumino, H., Nagao, K., 2009. Retroarc volcanism in the northern San Rafael Block (34°–35° 30′S), southern Central Andes: occurrence, age, and tectonic setting. J. Volcanol. Geotherm. Res. 186, 169–185.

Forasiepi, A., Martinelli, A.G., Marcelo, S., Dieguez, S., Bond, M., 2011. Paleontology and stratigraphy of the Aisol Formation (Neogene), San Rafael, Mendoza. In: Salfity, J.A., Marquillas, R.A. (Eds.), Cenozoic Geology of the Central Andes of Argentina. SCS Publisher, Salta, pp. 135–154.

Franzese, J.R., Spalletti, L.A., 2001. Late Triassic–early Jurassic continental extension in southwestern Gondwana: tectonic segmentation and pre-break-up rifting. J. S. Am. Earth Sci. 14, 257–270.

Galindo, I., Gudmundsson, A., 2012. Basaltic feeder dykes in rift zones: geometry, emplacement and effusion rates. Nat. Hazards Earth Syst. Sci. 12, 3683–3700.

Germa, A., Quidelleur, X., Gillot, P.Y., Tchilinguirian, P., 2010. Volcanic evolution of the back-arc Pleistocene Payun Matru volcanic field (Argentina). J. S. Am. Earth Sci. 29, 717–730.

Geshi, N., Kusumoto, S., Gudmundsson, A., 2010. Geometric difference between non-feeder and feeder dikes. Geology 38 (3), 195–198.

Geyer, A., Martí, J., 2010. The distribution of basaltic volcanism on Tenerife, Canary Islands: implications on the origin and dynamics of the rift systems. Tectonophysics 483, 310–326.

Giambiagi, L., Bechis, F., García, V., Clark, A.H., 2008. Temporal and spatial relationships of thick- and thin-skinned deformation: a case study from the Malargüe fold-and-thrust belt, southern Central Andes. Tectonophysics 459, 123–139.

Giambiagi, L., Ghiglione, M., Cristallini, E., Bottesi, G., 2009. Características estructurales del sector sur de la Faja Plegada y Corrida de Malargüe (35°–36° S): Distribución del acortamiento e influencia de estructuras previas. Rev. Asoc. Geol. Argent. 65 (1), 140–153.

González Díaz, E., 1972. Descripción geológica de la Hoja 30^{d}, Payún Matrú. Dirección Nacional de Geología y Minería, Boletín, 130 (Buenos Aires).

Gudmundsson, A., 1995. Stress field associated with oceanic transform faults. Earth Planet. Sci. Lett. 136, 603–614.

Gudmundsson, A., 2000. Dynamics of volcanic systems in Iceland: example of tectonism and volcanism at juxtaposed hot spot and mid-ocean ridge systems. Annu. Rev. Earth Planet. Sci. 28, 107–140.

Gudmundsson, A., 2006. How local stresses control magma-chamber ruptures, dyke injections, and eruptions in composite volcanoes. Earth Sci. Rev. 79, 1–31.

Gudmundsson, A., 2007a. Conceptual and numerical models of ring-fault formation. J. Volcanol. Geotherm. Res. 164, 142–160.

Gudmundsson, A., 2007b. Infrastructure and evolution of ocean-ridge discontinuities in Iceland. J. Geodyn. 43, 6–29.

Gudmundsson, A., 2011. Rock Fractures in Geological Processes. Cambridge University Press, New York.

Gudnason, J., Holm, P.M., Søager, N., Llambías, E.J., 2012. Geochronology of the late Pliocene to recent volcanic activity in the Payenia back-arc volcanic province, Mendoza Argentina. J. S. Am. Earth Sci. 37, 191–201.

Guzmán, C.G., Cristallini, E.O., Bottesi, G.L., 2007. Contemporary stress orientations in the Andean retroarc between 34° S and 39° S from borehole breakout analysis. Tectonics 26, 1–13 (TC3016).

Guzmán, C.G., Cristallini, E.O., García, V.H., Yagupsky, D.L., Bechis, F., 2011. Evolución del campo de esfuerzos horizontal desde el Eoceno a la actualidad en la Cuenca Neuquina. Rev. Asoc. Geol. Argent. 68 (4), 542–554.

Hernando, I.R., Llambías, E.J., González, P.D., Sato, K., 2012. Volcanic stratigraphy and evidence of magma mixing in the Quaternary Payún Matrú volcano, Andean backarc in western Argentina. Andean Geology 39 (1), 158–179.

Howell, J.A., Schwarz, E., Spalletti, L.A., Veiga, G.D., 2005. The Neuquén Basin: an overview. In: Veiga, G.D., Spalletti, L.A., Howell, J.A., Schwarz, E. (Eds.), The Neuquén Basin, Argentina: A Case Study in Sequence Stratigraphy and Basin Dynamics. Geological Society, Special Publication, 252, pp. 1–14. The Geological Society of London, London.

Kay, S.M., Burns, W.M., Copeland, P., Mancilla, O., 2006. Upper Cretaceous to Holocene magmatism and evidence for transient Miocene shallowing of the Andean subduction zone under the northern Neuquén Basin. In: Kay, S.M., Ramos, V.A. (Eds.), Evolution of an Andean Margin: A Tectonic and Magmatic View From the Andes to the Neuquén Basin (35°–39° S Latitude). Geological Society of America, Special Paper, 407, pp. 19–60. Geological Society of America, Colorado.

Legarreta, L., Uliana, M.A., 1991. Jurassic–Cretaceous marine oscillations and geometry of a back-arc basin fill, central Argentine Andes. In: MacDonald, D.I.M. (Ed.), Sedimentation, Tectonics and Eustacy. Sea Level Changes at Active Margins. International Association of Sedimentologists, Special Publications, 12, pp. 429–450.

Lipman, P.W., 2000. Calderas, in: Sigurdsson, H. (Ed.), Encyclopedia of Volcanoes. Academic Press, California, pp. 643–662.

Llambías, E.J., 1966. Geología y petrología del volcán Payún Matrú, Mendoza. Acta Geológica Lilloana 7 (San Miguel de Tucumán).

Llambías, E.J., Kleiman, L.E., Salvarredi, J.A., 1993. El magmatismo gondwánico. In: Ramos, V.A. (Ed.), 12° Congreso Geológico Argentino and 2° Congreso de Exploración de Hidrocarburos, pp. 53–64.

Llambías, E.J., Bertotto, G.W., Risso, C., Hernando, I.R., 2010. El volcanismo cuaternario en el retroarco de Payenia: una revisión. Rev. Asoc. Geol. Argent. 67 (2), 278–300.

Manceda, R., Figueroa, D., 1995. Inversion of the Mesozoic Neuquén rift in the Malargüe fold and thrust belt, Mendoza, Argentina. In: Tankard, A.J., Suárez, S., Welsink, H.J. (Eds.), Petroleum Basins of South America. AAPG Memoir, 62, pp. 369–382.

Mazzarini, F., Fornaciai, A., Bistacchi, A., Pasquarè, F.A., 2009. Fissural volcanism, polygenetic volcanic fields, and crustal thickness in the Payén Volcanic Complex on the central Andes foreland (Mendoza, Argentina). Geochem. Geophys. Geosyst. 9 (9). http://dx.doi.org/10.1029/2008GC002037.

Meijer, P., 1997. Forces controlling the present day state of stress in the Andes. World Stress Map Rel. 1997-1Heidelberg Academy of Sciences and Humanities.

Morley, C.K., 1995. Developments in the structural geology of rifts over the last decade and their impact on hydrocarbon exploration. In: Lambiase, J.J. (Ed.), Hydrocarbon Habitat in Rift Basins. Geological Society, Special Publication, 80, pp. 1–32. The Geological Society of London, London.

Nakamura, K., 1977. Volcanoes as possible indicators of tectonic stress orientation — principle and proposal. J. Volcanol. Geotherm. Res. 2, 1–16.

Németh, K., Martin, U., 2007. Shallow sill and dyke complex in western Hungary as a possible feeding system of phreatomagmatic volcanoes in “soft rock” environment. J. Volcanol. Geotherm. Res. 159, 138–152.

Ostera, A.H., Dapeña, C., 2003. Environmental isotopes and geochemistry of Bañado Carilauquén, Mendoza, Argentina. Short Papers, 4th South American Symposium on Isotope. Geology, pp. 461–464.

Pángaro, F., Pereira, D.M., Micucci, E., 2009. El sinrift de la Dorsal de Huincul, Cuenca Neuquina: Evolución y control sobre la estratigrafía y estructura del área. Rev. Asoc. Geol. Argent. 65 (2), 265–277.

Parfitt, E., Wilson, L., 2008. Fundamentals of Physical Volcanology. Blackwell, Oxford.

Paulsen, T.S., Wilson, T.J., 2010. New criteria for systematic mapping and reliability assessment of monogenetic volcanic vent alignments and elongate volcanic vents for crustal stress analyses. Tectonophysics 482, 16–28.

Petrinovic, I.A., Riller, U., Brod, J.A., Alvarado, G., Arnosio, M., 2006. Bimodal volcanism in a tectonic transfer zone: evidence for tectonically controlled magmatism in the southern Central Andes, NW Argentina. J. Volcanol. Geotherm. Res. 152, 240–252.

Polanski, J., 1954. Rasgos geomorfológicos del territorio de la provincia de Mendoza. Cuadernos de Estudio e Investigación, 4. Ministerio de Economía del Gobierno de Mendoza, Instituto de Investigaciones Económicas y Tecnológicas, pp. 4–10.

Quidelleur, X., Carlut, J., Tchilinguirian, P., Germa, A., Gillot, P.Y., 2009. Paleomagnetic directions from mid-latitude sites in the southern hemisphere (Argentina): contribution to time averaged field models. Phys. Earth Planet. Inter. 172, 199–209.

Ramos, V.A., 1978. Estructura. Congreso Geológico Argentino, Geología and Recursos Naturales del Neuquén, 7, Relatorio, pp. 99–118.

Ramos, V.A., Folguera, A., 2011. Payenia volcanic province in the Southern Andes: an appraisal of an exceptional Quaternary tectonic setting. J. Volcanol. Geotherm. Res. 201, 53–64.

Ramos, V.A., Kay, S.M., 2006. Overview of the tectonic evolution of the southern Central Andes of Mendoza and Neuquén (35°–39°S latitude). In: Kay, S.M., Ramos, V.A. (Eds.), Evolution of an Andean Margin: A Tectonic and Magmatic View From the Andes to the Neuquén Basin (35°–39°S Latitude). Geological Society of America, Special Paper, 407, pp. 1–17. Geological Society of America, Colorado.

Ramsey, J.M., Chester, F.M., 2004. Hybrid fracture and the transition from extension fracture to shear fracture. Nature 428, 63–66.

Rodríguez, E., Morris, C.S., Belz, J.E., Chapin, E.C., Martin, J.M., Daffer, W., Hensley, S., Rodríguez, E., Morris, C.S., Belz, J.E., Chapin, E.C., Martin, J.M., Daffer, W., Hensley, S., 2005. An assessment of the SRTM topographic products. Technical Report JPL D-31639. Jet Propulsion Laboratory.

Rossello, E.A., Cobbold, P.R., Diraison, M., Arnaud, N., 2002. Auca Mahuida (Neuquén Basin, Argentina): a Quaternary shield volcano on a hydrocarbon-producing substrate. 5th International Symposium on Andean Geodynamics, Toulouse, Extended Abstracts, pp. 549–552.

Sagripanti, L., Bottesi, G., Kietzmann, D., Folguera, A., Ramos, V.A., 2012. Mountain building processes at the orogenic front. A case study of the unroofing in Neogene foreland sequence (37° S). Andean Geology 39 (2), 201–219.

Silvestro, J., Atencio, M., 2009. La cuenca Cenozoica del Río Grande y Palauco: Edad, evolución y control estructural, Faja Plegada de Malargüe (36° S). Rev. Asoc. Geol. Argent. 65 (1), 154–169.

Silvestro, J., Kraemer, P., Achilli, F., Brinkworth, W., 2005. Evolución de las cuencas sinorogénicas de la Cordillera Principal entre 35°–36° S, Malargüe. Rev. Asoc. Geol. Argent. 60 (4), 627–643.

Soria, M.F., 1983. Vertebrados fósiles y edad de la Formación Aisol, provincia de Mendoza. Rev. Asoc. Geol. Argent. 38 (3–4), 299–306.

Takada, A., 1994. The influence of regional stress and magmatic input on styles of monogenetic and polygenetic volcanism. J. Geophys. Res. 99 (B7), 13563–13573.

Tibaldi, A., 1995. Morphology of pyroclastic cones and tectonics. J. Geophys. Res. 100 (B12), 24521–24535.

Tibaldi, A., Pasquarè, F., Tormey, D., 2010. Volcanism in reverse and strike–slip fault settings. In: Cloetingh, S., Negendank, J. (Eds.), New Frontiers in Integrated Solid Earth Sciences. International Year of Planet Earth. http://dx.doi.org/10.1007/978-90-481-2737-5_9. Springer Science+Business Media B.V.

Turienzo, M.M., Dimieri, L.V., Frisicale, M.C., Araujo, V.S., 2010. Evolución de las estructuras andinas en la región del Río Diamante (34°40′LS): Vinculación entre la Faja Corrida y Plegada de Malargüe y la Cordillera Frontal. Rev. Asoc. Geol. Argent. 67 (3), 354–368.

Vergani, G.D., Tankard, A.J., Belotti, H.J., Welsink, H.J., 1995. Tectonic evolution and paleogeography of the Neuquén Basin, Argentina. In: Tankard, A.J., Suárez Soruco, R., Welsink, H.J. (Eds.), Petroleum Basins of South America. AAPG Memoirs, 62, pp. 383–402.

Zapata, T., Folguera, A., 2005. Tectonic evolution of the Andean fold and thrust belt of the southern Neuquén Basin, Argentina. In: Veiga, G.D., Spalletti, L.A., Howell, J.A., Schwarz, E. (Eds.), The Neuquén Basin, Argentina: A Case Study in Sequence Stratigraphy and Basin Dynamics. Geological Society, London, Special Publications, 252 (1), pp. 37–56.